International Conference on Space Optics—ICSO 2018

Chania, Greece

9–12 October 2018

Edited by Zoran Sodnik, Nikos Karafolas, and Bruno Cugny

Broadband antireflection coatings for visible and infrared ranges

F. Lemarquis

T. Begou

J. Ruscica

D. Turover

et al.

International Conference on Space Optics — ICSO 2018, edited by Zoran Sodnik, Nikos Karafolas, Bruno Cugny, Proc. of SPIE Vol. 11180, 1118043 · © 2018 ESA and CNES · CCC code: 0277-786X/18/$18 · doi: 10.1117/12.2536066

Broadband antireflection coatings for visible and infrared ranges

F. Lemarquis[1], T. Begou[1], J. Ruscica[2], D. Turover[2] and J. Lumeau[1,*]
[1]Aix Marseille Univ, CNRS, Centrale Marseille, Institut Fresnel, F-13013 Marseille, France
[2]SILSEF, 382, rue Louis Rustin Archamps Technopole F-74160 Archamps, France

ABSTRACT

Antireflection coatings are among the most common and spread optical coatings that are used in every optical system in order to decrease losses and prevent shadow images. For space applications, they are critical elements which specifications will highly influence the overall optical systems performances. Despite the very wide range of developments that have been carried out over the past thirty years, the production of broadband antireflection coatings for visible and infrared ranges remains a challenge. In this paper, we will present some recent results based on thin film technology for the production of antireflection coatings dedicated to visible, near-IR and mid-IR spectral ranges. We will first present broadband antireflection coatings for [400-1100] nm spectral range We will present two type of coatings, one for normal and one for oblique incidence. Experimental demonstration by plasma assisted reactive magnetron sputtering using a Bühler HELIOS machine will be presented. We will then show antireflection coatings covering the [1.5-15] µm range. Experimental demonstration and limitation will be presented.

Keywords: optical coating, antireflection coatings, thin film design, physical vapor deposition.

1. INTRODUCTION

Antireflection coatings are among the most common and spread optical coatings that are used in every optical system in order to decrease losses and prevent shadow images. For space applications, they are critical elements which specifications will highly influence the overall optical systems performances. Despite the very wide range of developments that have been carried out over the past century [1-5], the production of broadband antireflection coatings for visible and infrared ranges remains a challenge. Actually, while optical coatings can, in theory, provide perfect antireflection function at a single wavelength, the final performances will then be highly affected by the spectral range of interest [2,6]. There are some various rules of thumb, when it comes to the design of antireflection coatings.

- The performances that can be achieved depend on the refractive index of the materials used in the design. The best results are obtained by using the lowest and highest possible indices. For this reason, the combination of SiO_2 and Nb_2O_5 (n ≈ 1.47 and 2.35) appears as the best solution for the visible, near-IR range, e.g. 400-1100 nm.
- The average residual reflection that can be achieved with multilayer structures depends on the required spectral range, the broader this range, the higher the residual reflection.
- If broader spectral range is needed and especially going down to 350 nm, due to the absorption of Nb_2O_5 in the UV range, Nb_2O_5 should be replaced with HfO_2 (n ≈ 2.05) to cover for example 350-1100 nm range. The refractive index being lower, and the spectral range extended, the residual reflection will then be higher. When it comes to extend the spectral range to longer wavelength, due to absorption of oxide materials above 2.5 µm, it is then required to use sulfide and/or fluorides materials. For this purpose, the use of ZnS and YF_3 appears as one of the most appropriate couple of materials available today. However, absorption of YF_3 in some spectral ranges will affect the coating performances within these ranges.
- The performances of antireflection treatments are indeed very sensitive to thickness variations of the layers. As a consequence, increasing the number of layers of a coating stack in order to theoretically improve its spectral performances might finally result in poorer performances than a simpler design. In conclusion, the production of high performances antireflection coatings requires an accurate control of the thickness of each of the layers of the stack.

*julien.lumeau@fresnel.fr; phone 33 672 289 061.

In this paper, we demonstrate the performances that can be achieved in the design and the fabrication of high performance broadband antireflection coatings with today's technology.

2. RESULTS AND DISCUSSIONS

Three types of antireflection coatings have been considered in this study:

- An antireflection coating for silica substrates optimized for normal incidence and covering the 400-1100 nm spectral range.
- An antireflection coating for silica substrates optimized for oblique incidence (0 to 45°) and covering the 400-900 nm spectral range.
- An antireflection coating for ZnSe substrates optimized for normal incidence and covering the 1.5-15 µm spectral range.

Below, we provide a description of the design, the fabrication and the limitations of each type of antireflection coatings.

2.1 Visible/Near-IR antireflection coating for normal incidence

The first antireflection coating that has been studied is an antireflection optimized for the spectral band between 400 and 1100 nm operating at normal incidence. For this study, we considered Nb_2O_5 as the high refractive index material and SiO_2 as the low refractive index material and fused silica as the substrate. The minimum number of layers required to achieve such performances is equal to ~10. With such a stack the average reflection coefficient is equal to ~1%. Increasing the number of layers of the stack allows slightly decreasing the residual reflection to a level of ~0.8%. Such a residual reflection coefficient is the lowest value that can be achieved with a multilayer structure (see first and second rules of thumb). In this paper, we considered a formula with 20 alternated high and low refractive index layers (Table 1).

Table 1. Layers thicknesses of visible/Near-IR antireflection coating for zero incidence.

Layer #	Material	Thickness, nm
	Silica substrate	
1	Nb_2O_5	5.0
2	SiO_2	74.2
3	Nb_2O_5	18.0
4	SiO_2	43.6
5	Nb_2O_5	38.2
6	SiO_2	15.4
7	Nb_2O_5	86.2
8	SiO_2	13.9
9	Nb_2O_5	38.8
10	SiO_2	47.5
11	Nb_2O_5	13.9
12	SiO_2	143.8
13	Nb_2O_5	9.1
14	SiO_2	56.7
15	Nb_2O_5	32.7
16	SiO_2	17.8
17	Nb_2O_5	86.0
18	SiO_2	17.9
19	Nb_2O_5	28.7
20	SiO_2	108.1

It can be seen that the formula has no periodicity as well as large variations in thickness (30× change). There are also very thin layers: the first layer has a thickness of 5 nm and 8 layers have thicknesses lower than 20 nm. Finally, such a structure is very sensitive to an error on the thickness of each layer. This means that fabricating such structures requires a very good control of the thickness of each of the layers.

The technology chosen to fabricate this structure was PARMS (Plasma Assisted Reactive Magnetron Sputtering) technology. The depositions were therefore carried out using the Bühler HELIOS machine within the *Espace Photonique* platform of *Institut Fresnel*. The control of the thickness of each of the layers was carried out using a Bühler OMS 5000 optical monitoring system interfaced with the HELIOS machine. Two different optical monitoring strategies were considered: one with a single test glass and one with multiple test glasses. Indeed, the HELIOS machine is equipped with a load-lock system that allows changing the test glass during the fabrication in between the deposition of two layers. To begin with, we considered the use of a single test glass to monitor the entire stack. Using a dedicated software for the determination of optimal optical monitoring strategy combined with a Virtual Deposition Process software, the following optical monitoring strategy was determined:

- layers 1 to 16: optical monitoring at 420 nm,
- layers 17 to 20: time monitoring.

Given the complexity of stack, the determination of an optimal strategy remains complex and no all-optical strategy (i.e. with no time monitored layers) could be found. Such a prototype of antireflection coating was fabricated on the HELIOS machine and the transmission spectrum was measured using a Perkin Elmer Lambda 1050 spectrophotometer (Figure 1).

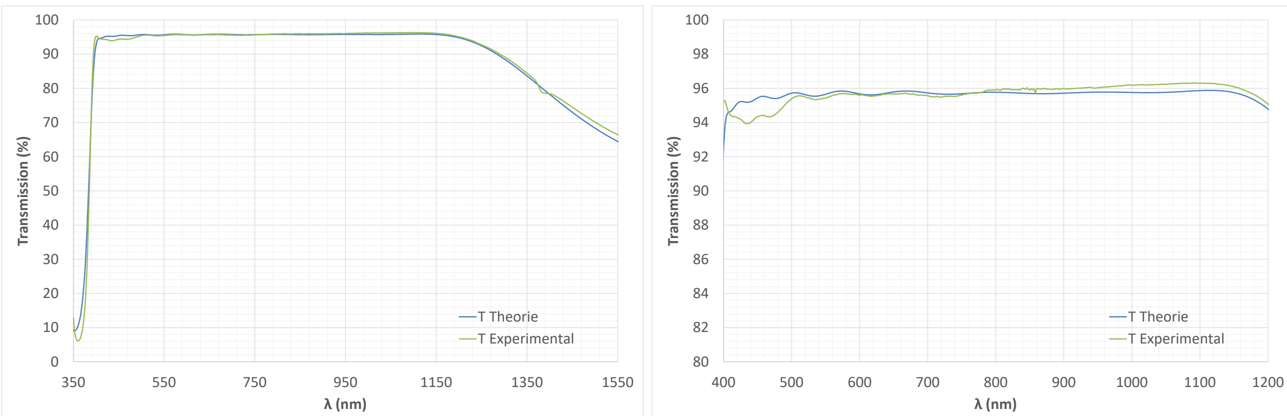

Fig. 1. Spectral transmission of visible/near-IR antireflection coating for normal incidence monitored with a single test glass.

We can first see that the proposed monitoring strategy allowed to precisely control the thickness of each layer. The overall performances are close to the theoretical one. However, it can be seen that there are some small disagreements on the short wavelength range, which are most certainly due to thickness errors in the last layers of the time-controlled stack. We therefore wondered whether it would be possible to further minimize production errors. In order to be able to generate an all-optical monitoring strategy, we opted for the use of two test glasses. A new optical monitoring strategy was therefore created:

- layers 1 to 8: optical monitoring at 410 nm on test glass 1,
- layers 9 to 20: optical monitoring at 470 nm on test glass 2.

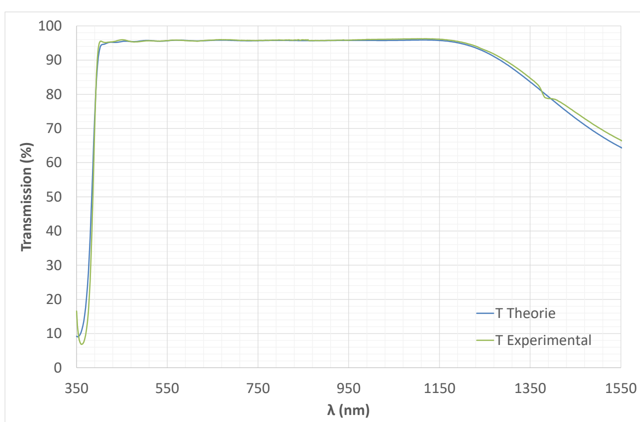

Fig. 2. Spectral transmission of visible/near-IR antireflection coating for normal incidence monitored with two test glasses.

We then fabricated a new prototype on the HELIOS machine using this new strategy. The transmission spectrum was then measured on this new component (Figure 2). It can be seen that using this method, we have been able to fabricate a visible/near-IR antireflection coating for normal incidence with very low manufacturing errors, thus making it possible to minimize the Fresnel reflection of a fused silica substrate with performances close to those predicted by the theory.

To further characterize the performances of the antireflection coatings and also test the repeatability of the manufacturing process, a new deposition run was performed (Run 2). Two types of samples were generated: a new single side antireflection coated sample and dual side antireflection coated samples (Run 1 + 2). The performances of the new single side antireflection coating were characterized and compared with the one of the first coating run (Figure 3).

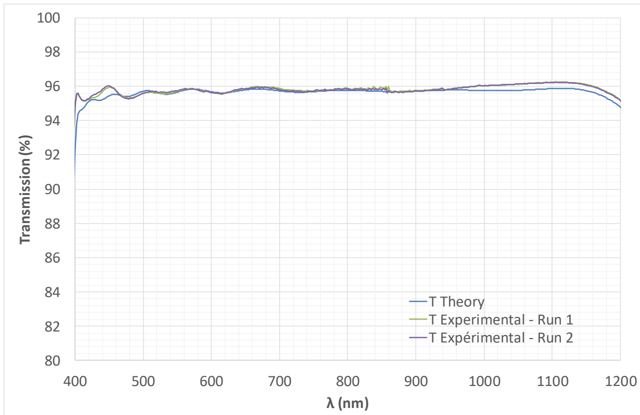

Fig. 3. Spectral transmission of visible/near-IR antireflection coating for normal incidence monitored with two test glasses. (Run 1 and 2).

It can be seen that the stability of the deposition rates of the HELIOS machine combined with the efficient developed optical monitoring strategy make it possible to guarantee optimal repeatability from one deposition to another. Finally, we measured the spectral response of the dual side component (Figure 4). It can be seen that the developed multilayer structures can guarantee an average reflectivity of the order of 98% with fluctuation not exceeding 1% over the spectral range 400-1100 nm.

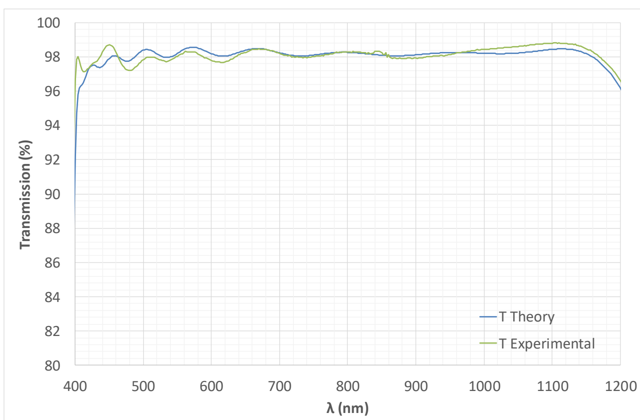

Fig. 4. Spectral transmission of dual side visible/near-IR antireflection coating for normal incidence monitored with two test glasses (depositions 1 and 2).

2.2 Visible/Near-IR antireflection coating for oblique incidence

The second antireflection coating structure that has been studied was optimized for the spectral band between 400 and 900 nm and allows minimizing the residual reflection at oblique incidence between 0 and 45°. In this particular case, the structure was optimized in order to minimize the residual reflection in S polarization. For this study, we again considered Nb_2O_5 as the high refractive index material and SiO_2 as the low refractive index material and fused silica as the substrate. The designed structure is given in Table 2. It is composed with 34 layers with a wide range of thicknesses. In this case, it is not possible to design more simple structures in order to achieve high performances. This can be easily explained by the fact that when the angle of incidence is increased, there is a blue shift of the whole spectrum that needs to be compensated by increasing the spectral range of the designed antireflection structure.

Table 2. Layers thicknesses of visible/Near-IR antireflection coating for oblique incidence.

Layer #	Material	Thickness, nm
	Silica substrate	
1	Nb_2O_5	5.3
2	SiO_2	70.1
3	Nb_2O_5	22.5
4	SiO_2	30.1
5	Nb_2O_5	79.5
6	SiO_2	11.4
7	Nb_2O_5	38.3
8	SiO_2	59.3
9	Nb_2O_5	6.8
10	SiO_2	146.0
11	Nb_2O_5	25.2
12	SiO_2	24.1
13	Nb_2O_5	76.2
14	SiO_2	35.4
15	Nb_2O_5	18.5
16	SiO_2	131.3
17	Nb_2O_5	17.0
18	SiO_2	37.1
19	Nb_2O_5	78.9
20	SiO_2	23.5
21	Nb_2O_5	23.9
22	SiO_2	142.3
23	Nb_2O_5	10.9
24	SiO_2	45.0
25	Nb_2O_5	79.0
26	SiO_2	13.7
27	Nb_2O_5	30.6
28	SiO_2	152.8
29	Nb_2O_5	3.2
30	SiO_2	55.7
31	Nb_2O_5	40.2
32	SiO_2	5.7
33	Nb_2O_5	72.2
34	SiO_2	104.2

Based on the results shown in Section 2.1 and in order to further minimize the errors of realization, we opted for an all optical monitoring strategy based on the use of three consecutive test glasses. A first test glass is used to monitor the first 12 layers, a second glass for the next 12 and a third glass for the last 10. We then determined the following monitoring strategy:

- layers 1 to 12: optical monitoring at 430 nm on test glass 1,
- layers 13 to 24: optical monitoring at 505 nm on test glass 2,
- layers 25 to 34: optical monitoring at 450 nm on test glass 3.

This strategy was then validated by performing simulations using Virtual Deposition Process software. We then made the deposition of the antireflection structure using the Bühler HELIOS machine. The transmission spectrum was finally measured at normal incidence (Figure 5).

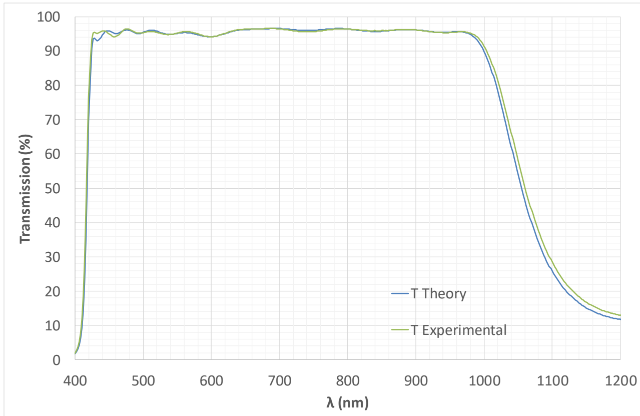

Fig. 5. Spectral response in transmission at normal incidence of a visible/near-IR antireflection coating optimized for S polarization in oblique incidence, deposited on one side, and optically monitored using 3 test glasses.

The transmission spectra were also measured at a 45° angle of incidence for the S and P polarizations (Figure 6). It should be noted that at a 45° angle of incidence, the reflection on the uncoated rear face induces a sharp decrease in the transmission of the order of 8% in S polarization while this contribution is negligible in polarization P (0.6%).

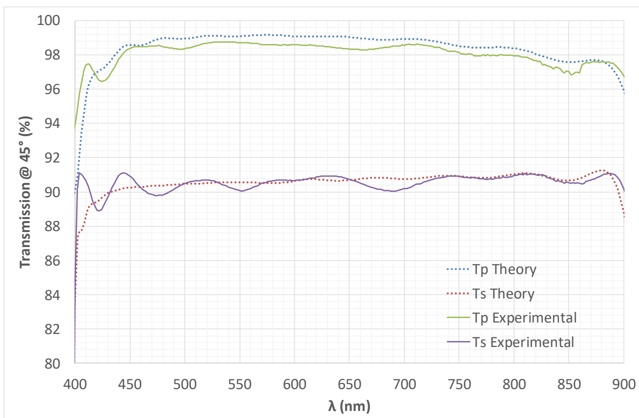

Fig. 6. Spectral response in transmission at a 45° angle of incidence of a visible/near-IR antireflection coating optimized for S polarization in oblique incidence, deposited on one side, and optically monitored using 3 test glasses.

We see that with this optical monitoring method, we have been able to minimize the errors on the layer thicknesses during the deposition of the coating, which guarantees a very good agreement between theory and experimental data.

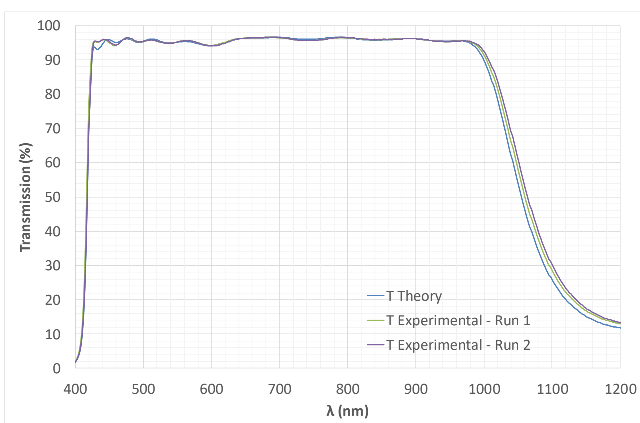

Fig. 7. Spectral response in transmission at normal incidence of visible/near-IR antireflection coating for oblique incidence monitored with three test glasses (Run 1 and 2).

We also repeated the manufacturing and monitoring process in order to fabricate dual-side coated samples. Figure 7 compares the transmission responses measured at normal incidence of the two coating runs. It can again be seen that the stability of the deposition rates of the HELIOS machine, combined with the optical monitoring process repeatability, ensures optimum repeatability from one deposition to another.

Finally, we measured the spectral response of the dual-side coated substrate (Figure 8). It can be seen that with these structures, it is possible to guarantee an average reflectivity of the order of 97% with fluctuations lower than 1.5% over the spectral range 400-900 nm. Transmission fluctuations a little larger than those predicted by the theory can be observed. This effect is probably due to a higher sensitivity of the stack, at oblique incidence, on deposition errors than at normal incidence.

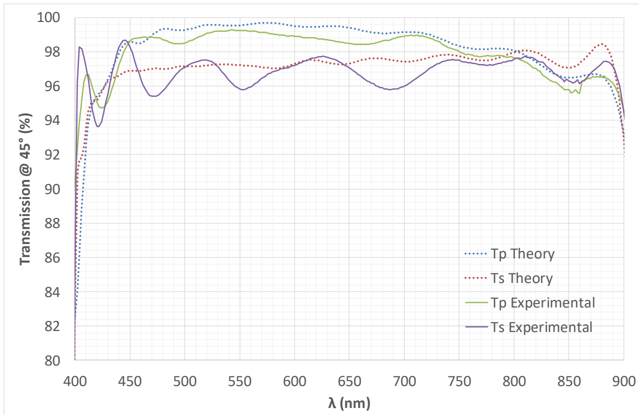

Fig. 8. Spectral response in transmission at a 45° angle of incidence of visible/near-IR antireflection coating for oblique incidence monitored with three test glasses (Run 1 and 2).

2.3 Near-IR/Mid-IR antireflection coating for normal incidence

The last antireflection coating structure that has been studied was optimized for the spectral band between 1.5 and 15µm and allows minimizing the residual reflection at oblique normal incidence. In this case, the chosen materials were no longer oxide materials but ZnS as the high refractive index material and YF_3 as the low refractive index material. The structure was optimized to minimize Fresnel reflection of a ZnSe substrate. The designed structure is given in Table 3. It is composed with 14 layers with thicknesses from 30 to 593 nm and a total thickness of 2.9 µm.

Table 3. Layers thicknesses of Near-IR/Mid-IR antireflection coating for normal incidence.

Layer #	Material	Thickness, nm
	ZnSe substrate	
1	ZnS	435.2
2	YF_3	30.8
3	ZnS	227.6
4	YF_3	74.1
5	ZnS	199.0
6	YF_3	121.5
7	ZnS	162.4
8	YF_3	176.4
9	ZnS	121.6
10	YF_3	234.9
11	ZnS	77.6
12	YF_3	308.3
13	ZnS	29.6
14	YF_3	593.5

The technology chosen to fabricate this structure is PIAD (Plasma Ion Assisted Deposition) technology. The depositions were therefore carried out using the Bühler SYRUSpro 710 machine within the *Espace Photonique* platform of *Institut*

Fresnel. The control of the thickness of each of the layers was carried out using a Bühler OMS 5000 optical monitoring system interfaced with the SYRUSpro machine. Using a dedicated software for the determination of optimal optical monitoring strategy combined with a Virtual Deposition Process software, the following optical monitoring strategy was determined:

- layers 1 to 6: optical monitoring at 720 nm,
- layers 7 to 14: optical monitoring at 740 nm.

We then made the deposition of the antireflection structure on a ZnSe substrate using the Bühler SYRUSpro 710 machine. The transmission spectrum was finally measured at normal incidence using a Fourier Transform Infrared Spectrometer (Figure 9).

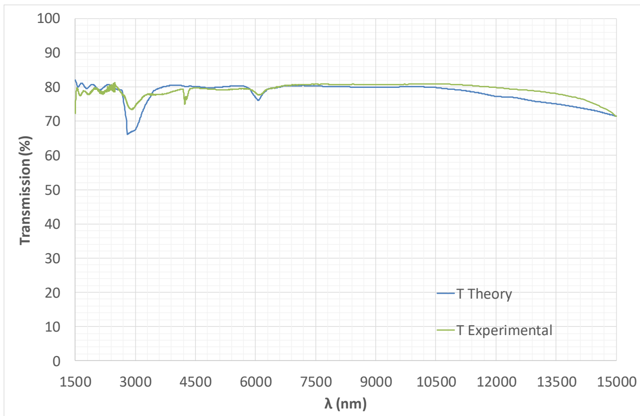

Fig. 9. Spectral response in transmission at normal incidence of a near-IR/mid-IR antireflection coating optimized normal incidence, deposited on one side of a ZnSe substrate.

One can see that using this strategy, we have been able to fabricate a broadband antireflection coating covering the whole 1.5-15 µm spectral range. There is a very good agreement between theory and experiment. It is also worth noting that the dispersion models that we used account for water absorption in near-IR ranges and also for long wavelength absorption, explaining the decrease of transmission in this wavelength range, not because of the design but because of the material properties. However, with such a structure, the average residual reflection on the coated surface is equal to about 3% and up to 5% at 15 µm. Using only a multilmayer structure, it is not possible to achieve lower residual reflection coefficient using these materials. In order to achieve further decrease of the residual reflection coeffient, it becomes mandatory to generate a gradient of refractive index at the boundary between the last layer of the stack and air. This can be achieved by structuring the last layer of the stack and adapting the design of the stack. Such activities are under development.

3. CONCLUSION

We have shown the design and the fabrication of broadband antireflection coatings for spectral ranges from visible up to mid-IR ranges. We have demonstrated that using multilayer structures, it is possible to design broadband antireflection structures that can be accurately manufactured using the proper optical monitoring strategy. We have also shown that the materials used for the design and the fabrication of such structures will highly influence the final performances of the antireflection coatings: increasing the spectral region where the antireflection is effective results in an increase of the residual reflection.

ACKNOWLEDGMENTS

This work was carried out within the framework of a Recherche et Technologie (R&T) project funded by the French Space Agency (CNES).

REFERENCES

[1] J. Strong, "On a Method of Decreasing the Reflection from Nonmetallic Substances," J. Opt. Soc. Am., 26, 1, 73–74 (1936).
[2] J. A. Dobrowolski and B. T. Sullivan, "Universal antireflection coatings for substrates for the visible spectral region," Appl. Opt. 35, 4993-4997 (1996).
[3] F. Lemarquis, G. Marchand, and C. Amra, "Design and manufacture of low-absorption ZnS–YF3 antireflection coatings in the 3.5–16-μm spectral range," Appl. Opt. 37, 4239-4244 (1998).
[4] J. A. Dobrowolski, Y. Guo, T. Tiwald, P. Ma, and D. Poitras, "Toward perfect antireflection coatings. 3. Experimental results obtained with the use of Reststrahlen materials," Appl. Opt. 45, 1555-1562 (2006).
[5] G. Tan, J.-H. Lee, Y.-H. Lan, M.-K. Wei, L.-H. Peng, I-C. Cheng, and S.-T. Wu, "Broadband antireflection film with moth-eye-like structure for flexible display applications," Optica 4, 678-683 (2017)
[6] T. V. Amotchkina, "Empirical expression for the minimum residual reflectance of normal- and oblique-incidence antireflection coatings," Appl. Opt. 47, 3109-3113 (2008).